Binary iron–carbon nanoparticle synthesis in photolysis of $Fe(CO)_5$ with methane and acetylene

A V Eremin, E V Gurentsov, E Yu Mikheyeva and S A Musikhin

Joint Institute for High Temperatures of the Russian Academy of Sciences, Izhorskaya 13 Bldg 2, Moscow 125412, Russia

E-mail: stasntsk@gmail.com

Abstract. The experimental investigation of iron–carbon nanoparticles synthesis by joint laser photolysis of iron pentacarbonyl in the mixture with methane or acetylene has been carried out. The radiation source used for photo-dissociation of precursors was a pulsed Nd:Yag laser operated at a wavelength of 266 nm. Under uv radiation the molecules of $Fe(CO)_5$ decomposed, forming atomic iron vapor and unsaturated carbonyls at well-known and readily controllable parameters. The subsequent condensation of supersaturated metal vapor resulted in small iron clusters and nanoparticles formation. It was assumed that the active catalytic surface of metal nanoparticles could activate the hydrocarbon molecules up to carbon layer formation on their surface. The growth process of the nanoparticles was observed by a method of laser light extinction. Additionally nanoparticle samples were investigated by a transmission electron microscope. The particle sizes were measured by microphotographs treatment. The sizes of synthesized particles from methane–iron-pentacarbonyl mixture were found to be in a range of 4–16 nm with a count median diameter of 8.9 nm and standard deviation of 1.13. These particles consisted of iron oxide without any carbon content. The particles formed in photolysis of acetylene–iron-pentacarbonyl mixture had the sizes of 3–7 nm with count median diameter of 4 nm and standard deviation of 1.28 and contained the essential amount of carbon. The iron cores were surrounded with a carbon shell.

1. Introduction

Metal-carbon nanoparticles promise a number of future applications in various fields of science and technology. An important feature of such particles is that metal core has magnetic and catalytic properties while carbon shell over metallic nanoparticles makes them resistant to oxidation and corrosion. On the other hand, a carbon shell over metallic nanoparticles allows an interaction with organic compounds for use in medical and biological applications. Metal-carbon nanoparticles can be used in the preparation of new materials for electronics (magnetic sensors, magnetic storage media, electronic and optoelectronic devices) [1]. Important potential application of metal-carbon nanoparticles may be their using as the targeted therapeutic agents delivery systems. Nanoparticles have high surface area to volume ratio. This allows for many functional groups to be attached to a nanoparticle, which can seek out and bind, for example, to certain tumor cells [2].

A number of different methodologies have been developed for the synthesis of carbon coated metal nanoparticles. The synthesis of iron–carbon nanoparticles was performed in shock-tube experiments at the co-pyrolysis of hydrocarbons (C_6H_6, C_3O_2, $CH_4 + C_3H_6O$) and iron pentacarbonyl ($Fe(CO)_5$) [3–5]. As a result of these studies, it was shown that it is possible

to synthesize the nanoparticles consisting of a metal core coated with a carbon coating. However, this would require conducting the synthesis process of two steps. First, performing the pyrolysis of iron pentacarbonyl behind incident shock wave at the temperatures of 500–900 K with iron particles formation, and second, pyrolysis of the carbonaceous material behind the reflected shock wave at higher temperatures (1600–1900 K) with the formation of iron–carbon nanoparticles.

One-step method of the synthesis of metal-carbon nanoparticles could be the pyrolysis (thermal decomposition) of carbonaceous and metallic substances in a thermal reactor at the uniform temperature. In [6] the synthesis of carbon coated silver nanoparticles based on silver nitrate and acetic acid pyrolysis was carried out.

Another type of the thermal reactor is the flame reactor. Yang and co-workers [7] have used a diffusion flame system to generate an aerosol of soot and iron oxide nanoparticles. The primary fuel was ethylene. Iron was introduced by passing ethylene over liquid iron pentacarbonyl. The iron appeared as crystals of Fe_2O_3, spatially segregated from the soot.

Nanoparticles of different materials can be obtained by using laser systems with various pulse durations, shapes, wavelengths, and fluences. For example, nanoparticles can be produced by ultra-short femtosecond laser pulses by target ablation in the presence of liquid. In [8] it was shown, that the ablation process over several nanoseconds resulted in the nanoparticle formation from the ablated metastable liquid layer, whereas only a minority is formed by condensation inside the cavitation bubble. Using hydrocarbons as liquid the carbon encapsulated metal nanoparticles could be synthesized.

One more method of thermal decomposition of gaseous precursors is their laser pyrolysis by a powerful infrared radiation. In study by Jager *et al* [9], the nanoparticles were synthesized under the influence of CO_2 laser on a gas mixture of iron pentacarbonyl and methylbenzene (CH_3–C_6H_5) with argon. To transmit laser energy to the molecules of precursors that do not have absorption bands in the wavelength of the laser radiation (10.6 μm) the authors used additives of ethylene, which absorbs the laser energy and collisionally transmits it to molecules of CH_3–C_6H_5 and $Fe(CO)_5$. As a result of the application of continuous laser power of 70 W, focused in the 2 mm spot in the stream of gas containing precursors, there is a region with a temperature high enough for the pyrolysis. Under these conditions the formed iron–carbon nanoparticles consisted partly of iron carbide (Fe_3C) and partly of iron oxides (Fe_2O_3, Fe_3O_4). In work [10] the co-decomposition of gaseous mixtures of silacyclopent-3-ene and $Fe(CO)_5$ by irradiation from two CO_2 lasers is reported. As a result the nanosized (α-Fe)-based particles that consist of both superparamagnetic and ferromagnetic phases were produced. They were enveloped within a thin graphitic shell and embedded in an organosilicon polymer matrix.

Additionally, the arc plasma and microwave plasma methods could be applied for binary metal-carbon particles synthesis. For example, the copper nanoparticles were synthesized by a modified arc plasma method using methane as carbon source [11]. ZrO_2 nanoparticles coated by Al_2O_3, Fe_2O_3 particles coated with ZrO_2 and Fe_2O_3 particles coated with polymer were obtained in microwave plasma reactor [12].

Method of uv photolysis of gaseous precursors for the synthesis of nanoparticles was developed previously [13–17]. The main advantage of this method is the minimum energy consumption due to selective contribution of laser energy to break chemical bonds of precursor molecules for producing the supersaturated vapor of atoms or active radicals which fast condense to nanoparticles. Besides, the photolytic dissociation method is a non-thermal process performed at room temperature. Therefore, the process of synthesis proceeds at ambient temperatures ensures no metal reactions with carbon forming carbides, which occur efficiently at high temperatures and are typical for other methods of synthesis. Metallocenes, such as ferrocene ($Fe(cp)_2$), nickelocene ($Ni(cp)_2$) and cobaltocene ($Co(cp)_2$) have been used as precursors for the formation of metal-containing carbon nanoparticles in work [14]. C_3O_2 and $Fe(CO)_5$ were investigated in

details as photo-dissociation precursors for carbon and iron particles formation elsewhere [15,16]. In [17], the iron–carbon nanoparticles were synthesized from the mixture of CCl_4 and $Fe(CO)_5$.

Besides the gaseous precursors, the laser irradiation of liquid precursors could be also applied for producing of iron containing carbon nanoparticles. Uv laser with 266-nm wavelength radiation of a mixture of ferrocene and carbon dioxide at low temperature was applied in [18]. Uv lasers of wavelengths ranging from 193 to 355 nm have been used for the photolysis of ferrocene and the deposition of iron containing carbon nanoparticles [19]. In [20] a method for synthesizing of carbon-encapsulated magnetic nanoparticles (CEMNPs) is reported. In the proposed method, a solution containing various metalocenes dissolved in xylene is irradiated with a nanosecond pulsed ultraviolet laser at room temperature and atmospheric pressure. Upon the completion of irradiation, CEMNPs (Fe–C, Ni–C, Co–C) with diameters ranging from a few nanometers to about 300 nm are produced in the solution. Analyzing above experiments one can conclude that simple systems of metal carbonyls with different hydrocarbons hitherto were not used for carbon-metal nanoparticle producing by uv pulse photolysis. On the other hand, the binary nanoparticle formation process using different hydrocarbons is interesting as for practical as well for theoretical point of view.

The goal of this study is developing of a method of uv photolysis for synthesis of iron–carbon nanoparticles in gas phase using the mixtures of methane and acetylene with iron pentacarbonyl. Previously, decomposition of methane and acetylene on nano-dispersed iron catalyst was performed at elevated temperatures 400–700 °C [21, 22]. However, due to uv laser energy impact on the precursors and redistribution of this energy among the electronic excited states of photolysis products [23], keep in mind that some activation of hydrocarbons under uv radiation could be the case and taking into account the energy release during nanoparticle condensation [24] one can assume that hydrocarbon decomposition could take place on iron nanoparticle surface even at room temperature. The main idea of suggested method is the using of catalytic activity of firstly formed iron-based nanoclusters and nanoparticles for decomposition of hydrocarbon molecules on their surface and formation outer carbon layer around iron core at room temperature.

2. Experimental setup

The experiments on the synthesis of iron–carbon nanoparticles were performed at room temperature in a quartz reaction cell of 0.5 cm^3 in a volume, which was preliminarily evacuated up to the pressure of 10^{-3} mbar and then filled with a mixture of 20 mbar of $Fe(CO)_5$ vapor and 0.1–1 bar of methane or 0.5 bar C_2H_2 diluted by 0.5 bar of argon prepared in separate vessel. Thus the total pressure in the reactor was varied from 0.1 bar to 1 bar. As a source of photons for the photo-dissociation of molecules of precursors a pulsed Nd:Yag laser SOLAR LQ-129 operated at forth harmonic (266 nm) was used. The light energy meter Ophir PE25-S was applied to determine the energy of the radiation per pulse.

The experimental setup is shown in figure 1. The setup was equipped with light extinction diagnostics for monitoring the process of the condensed phase growth. A cw He-Ne laser operated at 633 nm was used as a light source. The attenuation of laser signal due to nanoparticles formation after the pulse of Nd:Yag (FWHM = 12 ns) laser was registered using a photo-diode THORLABS PDA10A-EC and recorded by digital oscilloscope.

The particles were collected after one pulse synthesis experiments. The copper grids for transmission electron microscopy covered by carbon net were placed on the bottom of the reactor and particles deposited on the grid under natural gravity during 15 min after the experiment. After that the quartz reactor was opened and cleaned by ethanol. The particle sizes were measured by microphotographs treatment, which were made by transmission electron microscope (TEM). The additional electron micro diffraction pattern (MD) from TEM gave the information about nanoparticles structure.

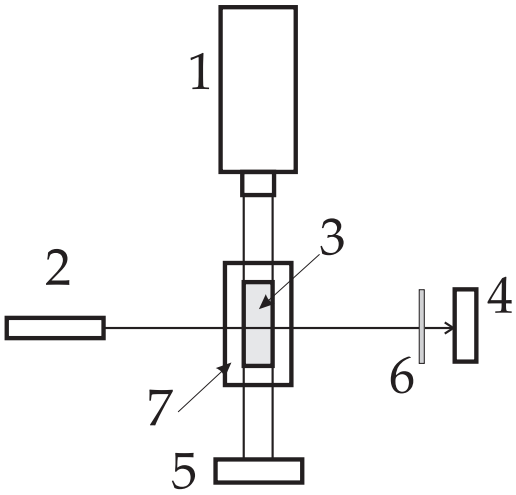

Figure 1. Experimental setup for the synthesis of iron–carbon nanoparticles: *1*—Nd:Yag laser; *2*—He-Ne laser for extinction measurements; *3*—quartz cell; *4*—photo-diode; *5*—energy meter; *6*—narrow-band pass optical filter 633 nm; *7*—flange on the bottom for evacuation and filling of reaction cell.

3. Extinction measurements of growing nanoparticles

The optical density of condensed phase D, characterizing the volume fraction of forming nanoparticles, was determined based on the Lambert-Beer law using the measured laser light extinction signal:

$$D = -\frac{\ln(I(t)/I_0)}{l}, \tag{1}$$

whereI_0 and I—the incoming and transmitted laser light intensities respectively, l—the optical path length. The light intensities are proportional to the signal amplitudes registered by scope. Thus, the ratio of amplitudes U/U_0 is equaled to the ratio of intensities I/I_0. Following the phenomenological description of the nanoparticle growth given in [16], we applied an equation of relaxation type for the description of the temporal variation of the optical density:

$$dD/dt = -k_{\text{eff}}(D_{\max} - D(t)), \tag{2}$$

where k_{eff}—the effective rate constant of condensed phase growth, $D_{\max}$—the maximum value of the optical density and t—the time. To extract the effective rate constant of condensed phase growth, the optical density time profiles were approximated by an exponential function derived from the equation (2):

$$D(t) = D_{\max}\left(1 - \exp\left(-k_{\text{eff}}t\right)\right). \tag{3}$$

Before addition of methane as a precursor for binary particle formation, the series of experiments in the mixture of $Fe(CO)_5$ + Ar has been performed. In figure 2 the optical density time profile obtained in one pulse photolysis of the mixture of 2% $Fe(CO)_5$ in Ar at the pressure of 1 bar is presented. An effective rate constant of particle growth derived by an approximation of experimental signal with exponential function was found to be $k_{\text{eff}} = 1.9 \times 10^4$ 1/s. That is in good agreement with the findings of [16] where the effective rate of iron particle growth was found to be $3{\times}10^4$ 1/s in the same mixture of 2% $Fe(CO)_5$ in Ar. The energy density per laser pulse was approximately the same in both experiments. The difference was in the less photon energy for photo-dissociation of $Fe(CO)_5$ in present study (266 nm) comparably 248 nm laser used in [16].

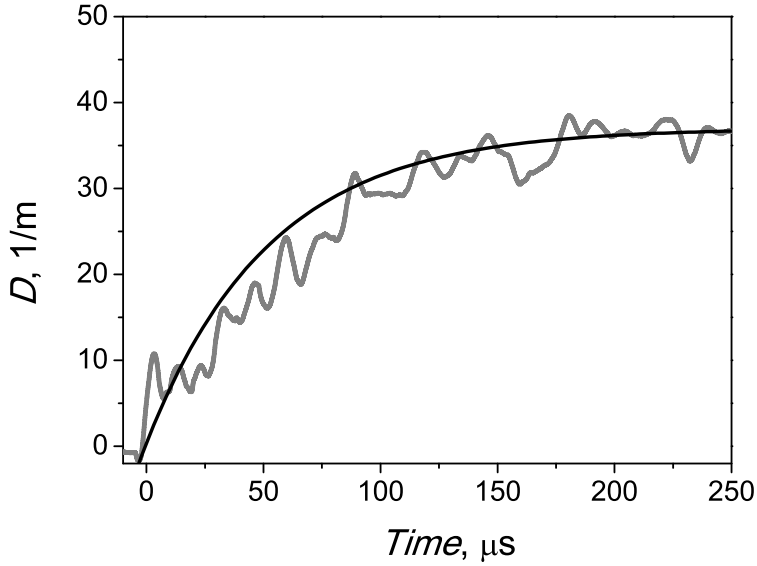

Figure 2. The optical density time profile obtained in one pulse photolysis of the mixture of 2% $Fe(CO)_5$ in Ar at the pressure of 1 bar (nosy curve) approximated by an exponential function derived from the equation (2) (smooth curve). The measurements were performed on the wavelength of 633 nm using a He-Ne laser.

4. Particle formation from $Fe(CO)_5$+CH_4 mixture

4.1. Results of extinction measurements

In figure 3 the optical density time profiles obtained in one pulse photolysis of the mixture of 2% $Fe(CO)_5$ in CH_4 are presented at different implemented pressures of 1 bar, 0.5 bar and 0.1 bar. These conditions corresponded to different precursor concentration at the same laser photolysis energy per pulse of 55 mJ passed through the front window of the reaction cell. An effective rate constant of particle growth derived by an approximation of experimental signals at the latter stage of particle growth during the time up to 200 μs was found to be 9×10^3 1/s at all three presented conditions which is twice less than that in the mixture of 2% $Fe(CO)_5$ in Ar at the same pressure and laser energy density. The difference in the effective particle growth rate in argon and methane could be explained by different cooling rate of forming nanopartilces. Admittedly that at this stage the rise of iron particle size proceeds by the addition of iron atoms and small clusters to larger particles. This mechanism is usually called as surface particle growth and it leads to increase of the volume fraction of condensed phase and, correspondingly, to the rise of optical density. During this process the heat of condensation, which releases onto condensed particles, is removed by the collisions with surrounding gas. Following to recommendations published by Sipkens and co-authors [25] the thermal energy accommodation coefficient of argon on iron nanoparticle surface could be higher than that of polyatomic gas like methane and could result in some overheating of growing nanoparticles in methane, leading to lower condensed phase growth rate. Since in figure 3 the latter stages of particle growth in the mixture of 2% $Fe(CO)_5$ are presented in the time scale of 200 μs the initial stages of this process taking about 1 μs are not resolved. These stages are shown in figure 4 in corresponding time scale. According to the data by Eremin et al [16] the process presented in figure 4 is the growth of small iron clusters which have the absorption bands in the vicinity of wavelength 615–633 nm. These iron clusters grow very quickly and could be considered as the initial centers of nanoparticle formation.

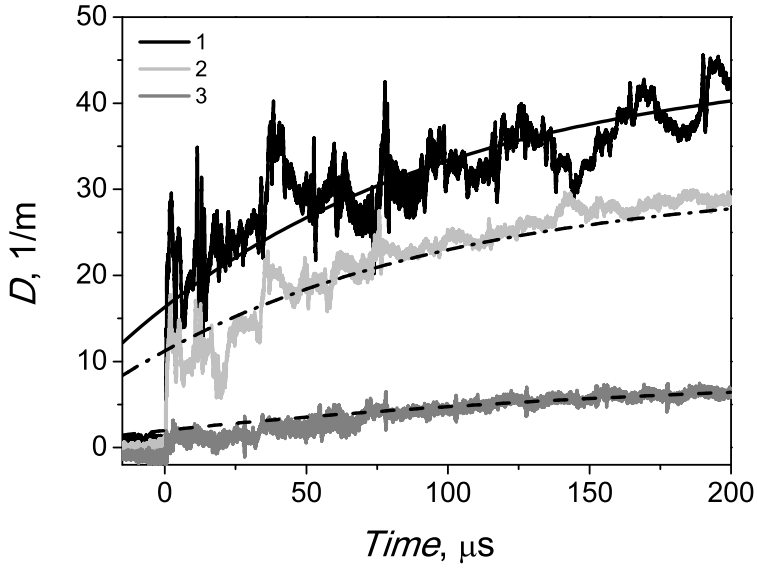

Figure 3. The time profiles of the optical density at 633 nm of the nanoparticles synthesized in the mixtures of 2% $Fe(CO)_5$ in CH_4 at various pressures: *1*—1 bar, *2*—0.5 bar, *3*—0.1 bar. Nosy curves—experimental data; smooth curves—the approximation of condensed phase growth rate by the exponential functions.

The values of the effective rate constant of iron clusters growth in the mixture of 2% $Fe(CO)_5$ in CH_4 were about 2×10^6 1/s which is an one order of magnitude less than the same value found in [16] for the mixture of 2% $Fe(CO)_5$ in Ar attained to 1.5×10^7 1/s. The lower rate of small iron cluster growth could be explained by less effectiveness of methane as a quenching partner of electronically excited iron atoms in comparison to argon [23, 26]. The quenching of excited iron atoms formed in photolysis of $Fe(CO)_5$ is a key mechanism of ground state atoms formation and following iron clusters growth.

It should be noted that the effective growth rate of condensed phase and the effective rate constant of iron clusters growth do not depend on the precursor concentration but depend on laser energy density. This phenomenon was pointed out by Emelianov et al [27].

Summary of the data of maximum value of optical density obtained in photolysis of the mixture of 2% $Fe(CO)_5$ in CH_4 at pressures of 1 and 0.5 bar versus laser fluence is presented in figure 5. The maximum values of optical density were measured at the times of 200–300 μs after the laser pulse when they had reached the final plateau. For comparison the data obtained in the mixture of 2% $Fe(CO)_5$ in Ar are presented as the asterisks. From figure 5 it is clearly seen that the maximum yield of condensed phase only dependent on the laser energy density implemented for photo-dissociation of $Fe(CO)_5$ and does not depend on the gas diluter. Thus, the difference of iron clusters growth rate in argon and methane at a short initial time period does not influence on the final value of optical density. It is known that methane molecule could not be dissociated at 266 nm even up to CH_3 radical and H atom in gas phase [28]. Therefore it is quite reasonable that the addition of methane instead of argon to $Fe(CO)_5$ has no influence on the dependence of maximum value of condensed phase on laser fluence. It means that in photolysis process the absorbed laser energy resulted only in photo-dissociation of $Fe(CO)_5$ and consequently to pure iron particle growth. Thus, one can conclude that the extinction measurements cannot present any evidences of the process of decomposition of methane molecules on the iron nanoparticle

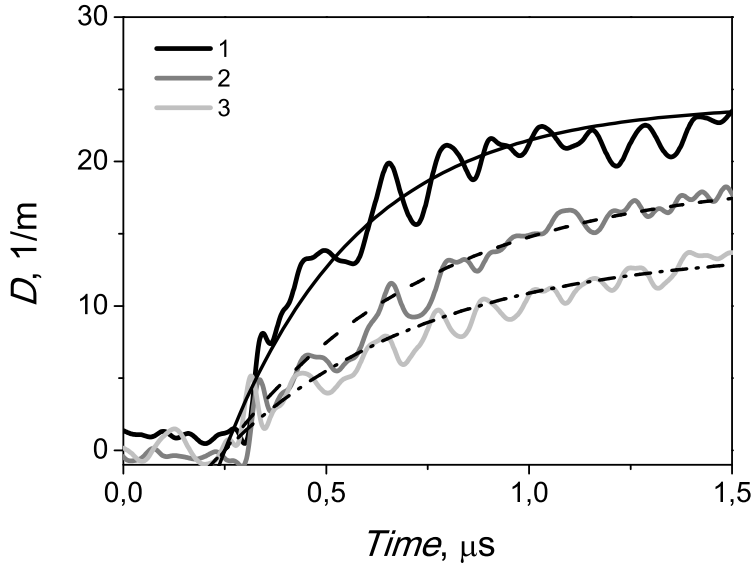

Figure 4. The initial stages of nanoparticle growth in the mixture of 1-bar CH_4 + 20-mbar $Fe(CO)_5$ at various pressures: *1*—0.9 bar; *2*—0.47 bar; *3*—0.44 bar. Nosy curves—the experimental signals; smooth curves—the approximations by exponential function (2).

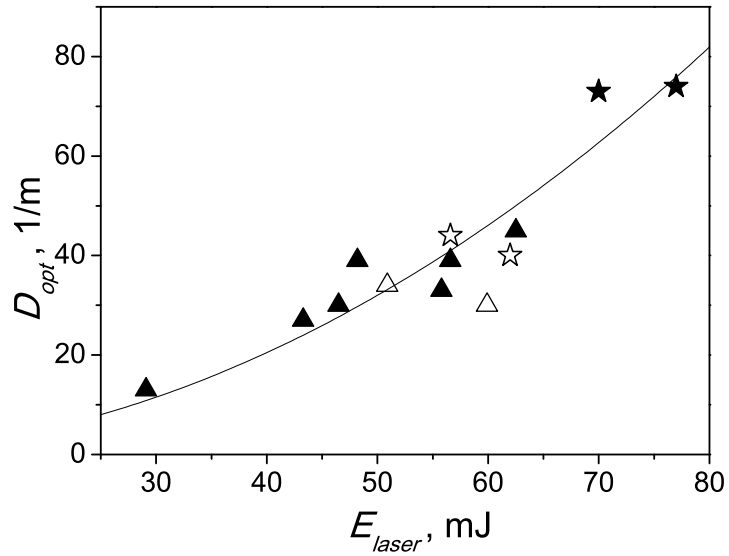

Figure 5. Maximal optical density of particles synthesized in the mixture of 20-mbar $Fe(CO)_5$ + 1-bar CH_4 (filled triangles) versus laser energy passed through the cell. Open symbols represent the same mixtures at the pressure of 0.5 bar. For the comparison the data in the mixture of 20-mbar $Fe(CO)_5$ + 1-bar Ar are presented as asterisks. Line—the best fit of experimental points.

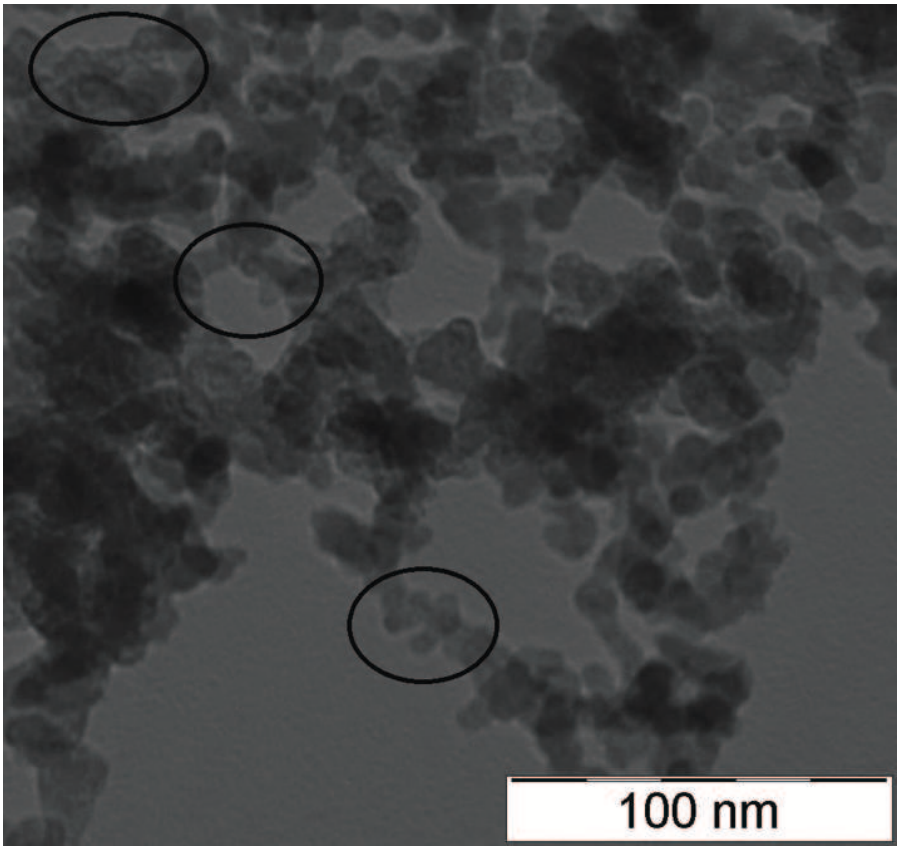

Figure 6. The micrographs of the synthesized nanoparticles in the mixture of 20-mbar $Fe(CO)_5$ + 1-bar CH_4.

surface at room temperature. However to get an ultimate answer on the question of the formation of carbon shell on the surface of iron nanoparticles one has to refer to results of analysis of particle samples performed by transmission electron microscope.

4.2. Results of TEM measurements

Examples of TEM images of nanoparticles obtained in the mixture of 20-mbar $Fe(CO)_5$ + 1-bar CH_4 are presented on figure 6. The more or less spherical primary particle agglomerates were found on all TEM images. Mostly the agglomerates have the structure like particle chains, but sometimes more dense structures were observed. Log-normal particle-size distribution was used for TEM particle sizing:

$$\mathrm{d}f = \frac{1}{\sqrt{2\pi} d_p \ln\sigma} \exp\left[\frac{(\ln d_p - \ln CMD)^2}{2(\ln\sigma)^2}\right] \mathrm{d}d_p. \tag{4}$$

where d_p—the current primary particle diameter, CMD—the count median diameter and σ—the standard deviation.

From figure 6 no evidence of iron encapsulated in carbon structure one can found as it was assumed previously. It is seen that some of primary nanoparticles are hollow inside (marked by circles in figure 6). This form could originate during the oxidation in air of the iron particles formed under inert atmosphere, when they were taken out from the reactor. It is known, that pure iron particles oxidize very fast at room temperature when they are exposed in air [29] even

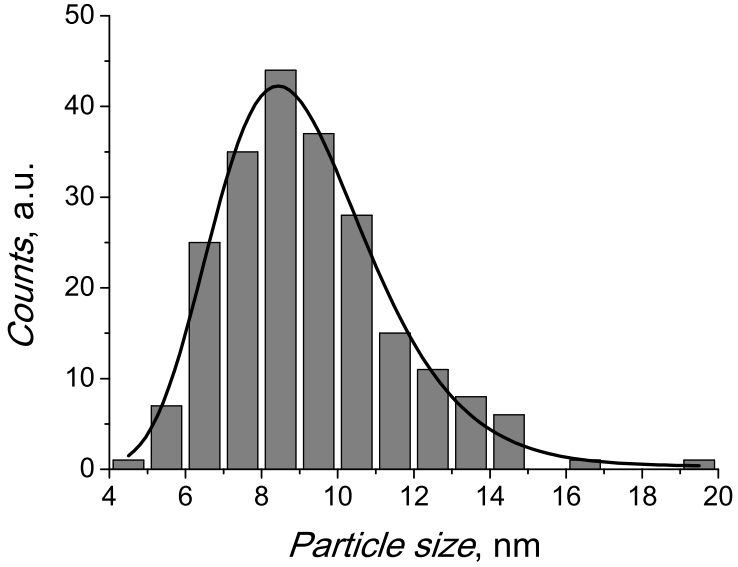

Figure 7. The histogram of particle size distribution synthesized in the mixture of 20-mbar $Fe(CO)_5$ + 1-bar CH_4 approximated by log normal function (4).

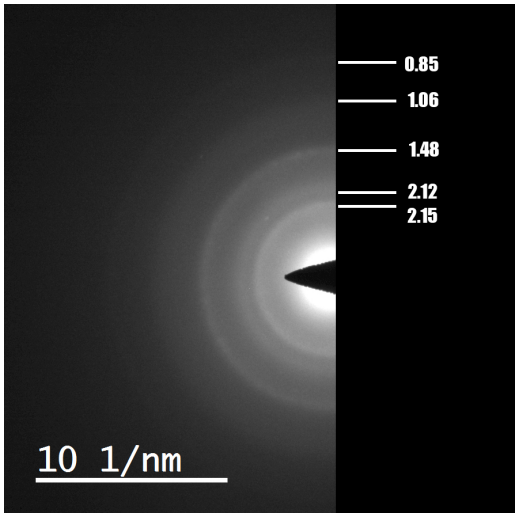

Figure 8. The electron micro-diffraction (MD) pattern of the samples of nanoparticles which was synthesized in the mixture of 20-mbar $Fe(CO)_5$ + 1-bar CH_4.

with void formation inside the particles. The statistical treatment of the microphotos related to photolysis of the mixture of 20-mbar $Fe(CO)_5$ + 1-bar of CH_4 presented in figure 7 has shown that the mean particle size is about 8.9 nm with standard deviation of 1.13 that is in good agreement with our previous work [16] devoted to pure iron particle formation.

The electron micro-diffraction analysis of the samples was performed to determine the composition of particles which had been analyzed by TEM. The typical MD pattern is shown in figure 8. The interplanar distances extracted from the rings of MD patterns were found to be 0.085 nm, 0.106 nm, 0.148 nm, 0.212 n, 0.215 nm. These values are in good agreement with

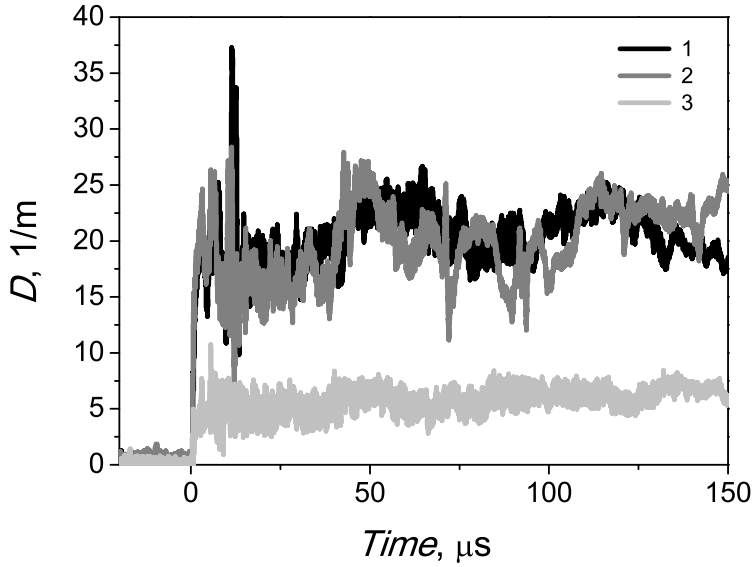

Figure 9. The time profiles of the optical density at 633 nm of the nanoparticles synthesized in the mixtures of 20-mbar $Fe(CO)_5$ + 0.5-bar C_2H_2 + 0.5-bar Ar at various pressures: *1*—1 bar, *2*—0.5 bar, *3*—0.1 bar. Laser energy—46 mJ.

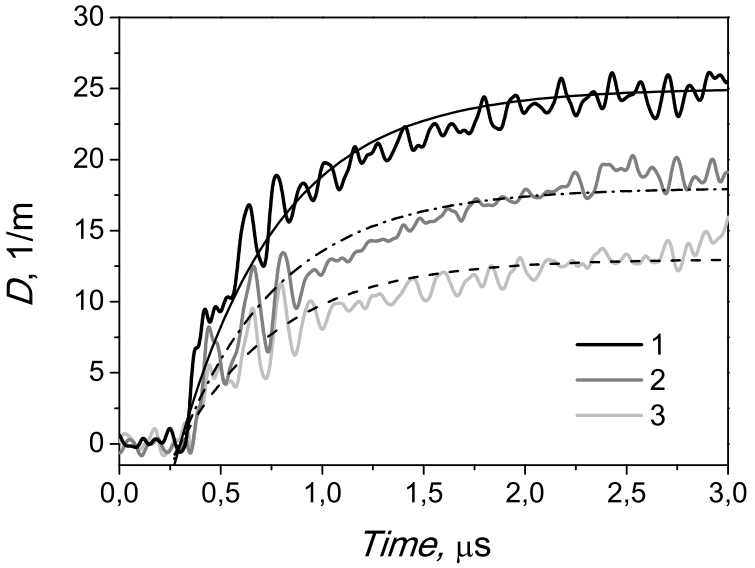

Figure 10. The initial stages of nanoparticle growth in the mixture of 20-mbar $Fe(CO)_5$ + 0.5-bar C_2H_2 + 0.5-bar Ar at various laser energies (*1*—59 mJ; *2*—49 mJ; *3*—39 mJ) at the pressure of the mixture of 1 bar. Noisy curves—the experimental signals; smooth curves—the approximation by exponential function (2).

data for hematite Fe_2O_3 (0.1056 nm, 0.1485 nm), magnetite Fe_3O_4 (0.0853 nm, 0.1483 nm, 0.210 nm) and wustite FeO (0.214 nm). The high temperature phases of iron and iron oxides were

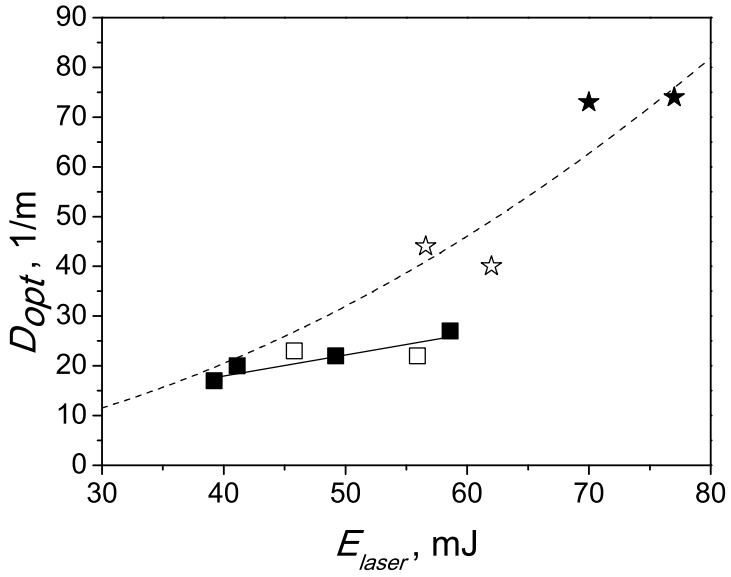

Figure 11. Maximum optical density of particles synthesized in the mixture of 2%$Fe(CO)_5$ + 49% C_2H_2 + 49% Ar (filled squares) versus laser energy passed through the cell. Dashed line–is the data fitting from figure 5. For comparison the data in the mixture of 20-mbar $Fe(CO)_5$ + 1-bar Ar are presented as asterisks. Open symbols represent the same mixtures at the pressure of 0.5 bar. Solid line shows the maximum optical density in the presence of acetylene.

not considered due to the near room temperature of particle synthesis. This conclusion is in good agreement with the study by Wang et al [29] in which the critical size of total oxidation of iron particles was found to be around 8 nm. Finally, one can conclude that in photolysis of the mixture of $Fe(CO)_5$ with methane only iron nanoparticles without carbon shell were synthesized.

5. Particle formation from $Fe(CO)_5$+C_2H_2 mixture

5.1. Extinction measurements results

In figure 9 the optical density time profiles measured in one pulse photolysis of the mixture of 2% $Fe(CO)_5$ + 49% C_2H_2 + 49% Ar at different pressures of 1 bar, 0.5 bar and 0.1 bar are presented. From this figure one can see that after a sharp increase of optical density during the first microsecond of process the particles do not demonstrate any trend to grow. On the other hand, at this secondary stage the growth of iron particle has to proceed by the addition of small clusters to larger particles as it was demonstrated by the time profiles of optical density shown in figures 2 and 3. Therefore, it is likely that the presence of activated acetylene molecules or their activation on the surface of iron clusters could lead to termination of the growth of condensed phase. In other words, the reason of the lack of observable raise of the optical density could be the covering of iron particles by carbon shell and changing of their resulting optical properties. The observed oscillations on the extinction signals are most likely originated by the non-uniform particles distribution over the reactor volume caused by the Gaussian laser spatial profile used for $Fe(CO)_5$ photo-dissociation.

In figure 10 the initial stages of nanoparticle growth in the mixture of 2% $Fe(CO)_5$ + 49% C_2H_2 + 49% Ar at various laser energies 39 mJ–59 mJ at the pressure of 1 bar are shown. The effective rate constants k_{eff} of iron clusters growth in this mixture was found to be dependent on the implemented laser energy. The values of k_{eff} were in the range 2.5–1.5$\times 10^6$ 1/s which are in

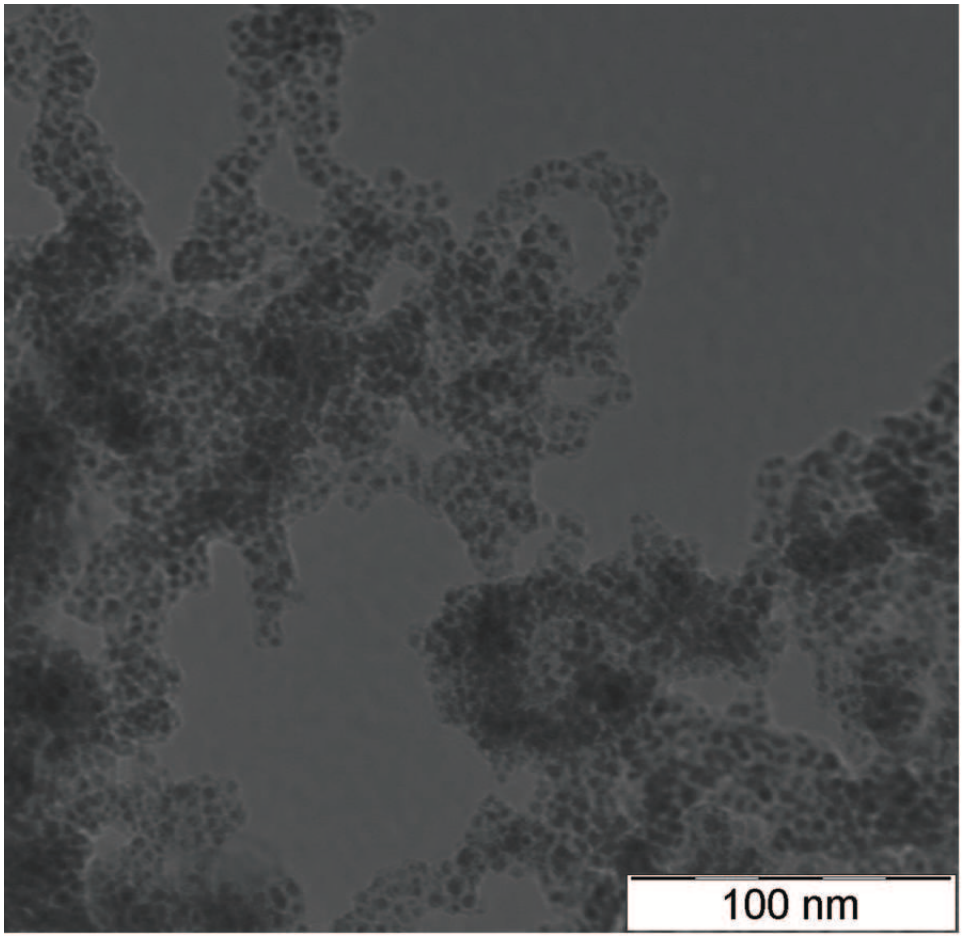

Figure 12. The micrograph of the synthesized nanoparticles in the mixture of 20-mbar $Fe(CO)_5$ + 0.5-bar C_2H_2 + 0.5-bar Ar.

good agreement with the values of k_{eff} found in the mixture of 2% $Fe(CO)_5$ in methane. Thus, the nanoparticle growth rate in the initial stages of nanoparticles growth in the photolysis of $Fe(CO)_5$ in methane and acetylene as the diluter gases proceeds similarly.

A summary of data of maximum optical density observed in photolysis of the mixture of 2%$Fe(CO)_5$ + 49% C_2H_2 + 49% Ar versus laser fluence is presented in figure 11. For comparison, the data observed in the mixture of 2%$Fe(CO)_5$ in methane, are presented in figure 11 by the dashed line and the data obtained in 2%$Fe(CO)_5$ with argon are presented as asterisks.

From figure 11 it is clearly seen that the maximum yield of condensed phase in the mixture of 2% $Fe(CO)_5$ + 49% C_2H_2 + 49% Ar (square symbols) does not noticeably increase at E_{laser} more than 42 mJ as compared with the yield of condensed phase in the mixture of 2% $Fe(CO)_5$ in CH_4 and in pure $Fe(CO)_5$ (asterisks). It could be explained that in the presence of acetylene in the mixture the carbon covering the iron clusters terminates their growth. Solid line in figure 11 shows the maximum optical density in the presence of acetylene. To get the direct evidence of the formation of carbon shell the results of analysis of particle samples performed by transmission electron microscope (TEM) have been considered.

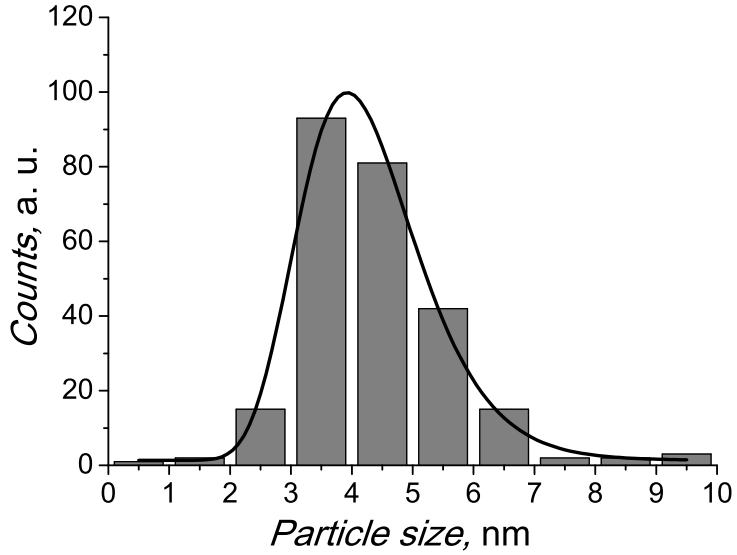

Figure 13. The histogram of particle size distribution synthesized in the mixture of 0.5-bar C_2H_2 + 20-mbar $Fe(CO)_5$ + 0.5-bar Ar approximated by log normal function (4).

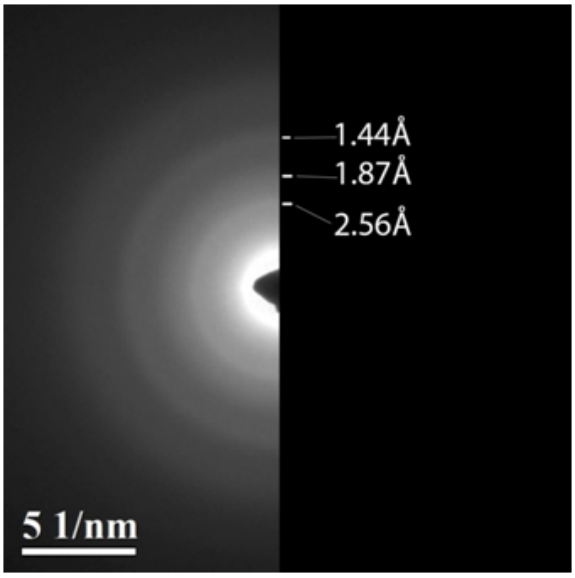

Figure 14. The electron micro-diffraction (MD) pattern of the samples of nanoparticles which were synthesized in the mixture of 0.5-bar C_2H_2 + 20-mbar $Fe(CO)_5$ + 0.5-bar Ar.

5.2. Results of TEM measurements

Example of TEM image of nanoparticles obtained in the mixture of 20-mbar $Fe(CO)_5$ + 0.5-bar C_2H_2 + 0.5-bar Ar is presented in figure 12. From figure 12 one can see that the particles formed in the mixture of 20-mbar $Fe(CO)_5$ + 0.5-bar C_2H_2 + 0.5-bar Ar consist of small dark nuclei surrounded or divided by light material. The particles on the TEM grid are combined in the aggregated chains. One can suppose that firstly formed small iron particles were later

covered by carbon shell. The histogram of particle size distribution obtained from statistical treatment of the microphotos from the mixture of 20-mbar $Fe(CO)_5$ + 0.5-bar C_2H_2 + 0.5-bar Ar is presented in figure 13. According to approximation of this distribution with the log-normal function (4) the mean particle size was found to be 4.16 nm with standard deviation of 1.28. Thus, in the mixture of 20-mbar $Fe(CO)_5$ + 0.5-bar C_2H_2 + 0.5-bar Ar the mean particle size is less than the pure iron nanoparticles formed in the mixture of $Fe(CO)_5$ with methane. As it was already mentioned above, the explanation of this fact could be the termination of the growth of iron particles growth due to covering them with carbon shell.

The typical MD pattern of extracted particles is shown in figure 14. The electron micro-diffraction pattern shows the interplanar distances 0.144 nm, 0.187 nm, 0.256 nm. These values are in good agreement with data for α-Fe (0.1433 nm), hematite Fe_2O_3 (0.184 nm) and magnetite Fe_3O_4 (0.253 nm). The limited number of visible rings in which one of them belongs to α-Fe and more diffusion pattern in comparison with figure 8 could be an evidence of presence of carbon shell surrounding iron clusters. However, in spite the carbon shell the iron core of the nanoparticles is partially oxidized. It could be a result of the amorphous structure of carbon shell.

6. Conclusions

Experimental investigations of the synthesis of nanoparticles were performed using activation of the mixtures of 2% $Fe(CO)_5$ in CH_4 and 2% $Fe(CO)_5$ + 49% C_2H_2 + 49% Ar by the pulse of Nd:Yag laser operated at 266 nm with laser energy up to 60 mJ per pulse. It was found that the photolysis of the mixture of 2% $Fe(CO)_5$ in CH_4 resulted in $Fe(CO)_5$ photo-dissociation without activation of methane molecules during the laser pulse. The measurements of condensed phase growth using laser light extinction in the mixture with methane resulted in good agreement with the previous data of iron particle growth in photolysis of $Fe(CO)_5$ in Ar. The results of transmission electron microscopy and micro-diffraction analysis of particles samples did not show carbon content in the particles synthesized in methane containing mixtures. The sizes of synthesized particles from methane–iron-pentacarbonyl mixture were found to be in a range of 4–16 nm with a count median diameter of 8.9 nm and standard deviation of 1.13. Thus, one can conclude that for using methane as a precursor for photo-synthesis of metal-encapsulated nanoparticles at room temperature it seems to be necessary to increase a laser fluence, or to impose the additional energy on the gas phase as heat, microwave, and so on, for activation or decomposition of methane molecules.

In contrast to that, the activation of the mixture of 2% $Fe(CO)_5$ + 49% C_2H_2 + 49% Ar by the same laser pulse with laser energy up to 60 mJ per pulse resulted in formation of binary iron–carbon nanoparticles. The iron cores were surrounded with carbon shell and sizes of resulted primary particles were found to be 3–7 nm with count median diameter of 4 nm and standard deviation of 1.28 and contained the essential amount of carbon. Thus, the acetylene in the mixture with $Fe(CO)_5$ is a good system for producing of carbon covered iron nanoparticles at room temperature by laser pulse photolysis at wavelength of 266 nm.

Acknowledgments

The authors sincerely acknowledge the financial support by grant from the Russian Science Foundation (No. 14-50-00124).

References

[1] Xia Y, Gates B, Yin Y and Lu Y 2000 *Adv. Mater.* **12** 693–770
[2] Emerich D F and Thanos C G 2006 *Biomol. Eng.* **23** 171–184
[3] Starke R, Kock B and Roth P 2003 *Shock Waves* **12** 351–361
[4] Gurentsov E, Eremin A, Roth P and Starke R 2005 *Kinet. Catal.* **46** 309–318

[5] Luo N, Chen T, Liu K and Shen Y 2013 *Mendeleev Commun.* **23** 153–154
[6] Scharmach W J, Sharma M K, Buchner R D, Papavassiliou V, Vajani G N and Swihart M T 2013 *AIChE J.* **59** 4116–4123
[7] Yang G, Teague S, Pinkerton K and Kennedy I M 2001 *Aerosol Sci. Technol.* **35** 759–766
[8] Povarnitsyn M E, Itina T E, Levashov P R and Khishchenko K V 2013 *Phys. Chem. Chem. Phys.* **15** 3108–3114
[9] Jager C, Mutschke H, Huisken F, Alexandrescu R, Morjan I, Dumitrache F, Barjega R, Soare I, David B and Schneeweiss O 2006 *Appl. Phys. A: Mater. Sci. Process.* **85** 53–62
[10] Daz L, Santos M, Ballesteros C, Maryko M and Pola J 2005 *J. Mater. Chem.* **15** 4311–4317
[11] Hao C, Xiao F and Cui Z 2008 *J. Nanopart. Res.* **10** 47–51
[12] Vollath D and Szab D V 1999 *J. Nanopart. Res.* **1** 235–242
[13] Huisken F, Kohn B, Alexandrescu R and Morjan I 1999 *Eur. Phys. J. D* **9** 141–144
[14] Elihn K, Landstrm L and Heszler P 2002 *Appl. Surf. Sci.* **186** 573–577
[15] Eremin A V, Gurentsov E V, Hofmann M, Kock B and Schulz C 2006 *J. Phys. D: Appl. Phys.* **39** 4359–4365
[16] Eremin A V, Gurentsov E V and Priemchenko K Y 2013 *J. Nanopart. Res.* **15** 1737
[17] Gurentsov E V and Eremin A V 2015 *Tech. Phys. Lett.* **41** 547–550
[18] Hasumura T, Fukuda T, Whitby R L D, Aschenbrenner O and Maekawa T 2011 *J. Nanopart. Res.* **13** 53–58
[19] Ouchi A, Tsunoda T, Bastl Z, Maryko M, Vorlicek V, Bohacek J, Vacek K and Pola J 2005 *J. Photochem. Photobiol., A* **171** 251–256
[20] Park J, Jeong S, Jeong M, Kim J and Cho B 2008 *Carbon* **46** 1369–1377
[21] Ibrahim A A, Fakeeha A H, Al-Fatesh A S, Abasaeed A E and Khan W U 2015 *Int. J. Hydrogen Energy* **40** 7593–7600
[22] Khedr M H, Halim K S A and Soliman N K 2008 *Appl. Surf. Sci.* **255** 2375–2381
[23] Mitchell S A and Hackett P A 1990 *J. Chem. Phys.* **93** 7813–7821
[24] Emelianov A, Eremin A, Makeich A, Jander H, Wagner H G, Starke R and Schulz C 2007 *Proc. Combust. Inst.* **31** 649–656
[25] Sipkens T A, Singh N R, Daun K J, Bizmark N and Ioannidis M 2015 *Appl. Phys. B: Lasers Opt.* **119** 561–575
[26] Gurentsov E V, Eremin A V and Priemchenko K Y 2013 *Tech. Phys.* **58** 1337–1345
[27] Emelianov A, Eremin A, Jander H and Wagner H G 2003 *Z. Phys. Chem.* **217** 1361–1368
[28] Okabe H 1978 *Photochemistry of Small Molecules* (John Wiley & Sons, New York)
[29] Wang C M, Baer D R, Thomas L E, Amonette J E, Antony J and Qiang Y 2005 *J. Appl. Phys.* **98** 094308